JOURNAL OF Applied Polymer SCIENCE

Essential Work of Fracture of Low-Filled Poly(methyl methacrylate)/ Starch Composites

S. Mohammad Ali,[1] G. Unnikrishnan,[2] M. A. Joseph[1]

[1]Department of Materials Science and Technology, National Institute of Technology, Calicut 673601, India

[2]Polymer Science and Technology Laboratory, National Institute of Technology, Calicut 673601, India

Correspondence to: S. Mohammad Ali (E-mail: smdali14@gmail.com)

ABSTRACT: In this study, poly(methyl methacrylate) (PMMA)/starch composites were prepared by a simple solvent casting method. The morphologies of the PMMA/starch composites were studied by scanning electron microscopy. The intermolecular interaction between PMMA and starch was investigated with Fourier transform infrared spectroscopy. The thermal properties of the PMMA/starch composites were compared with those of the pure PMMA sample. Thermogravimetric analysis showed that the thermal stability increased as the starch content increased in the composites. The biodegradability of the PMMA/starch composites was studied with a soil burial test. The degradability was measured in terms of mechanical strength, which increased as the starch content increased. The essential work of fracture (EWF) of the PMMA/starch composite films was investigated by the application of EWF theory under in-plane (mode I) conditions, and we found that the toughness, in terms of the EWF of composites, increased compared to that of pure PMMA. The fracture of the composites was also evaluated by ANSYS software, and the results were compared to the experimental output. The increased toughness of these PMMA/starch composites may enable their application in the automobile and packaging industries. © 2012 Wiley Periodicals, Inc. J. Appl. Polym. Sci. 000: 000–000, 2012

KEYWORDS: biodegradable; composites; simulations; thermogravimetric analysis (TGA); toughness

Received 20 November 2011; accepted 20 June 2012; published online

DOI: 10.1002/app.38230

INTRODUCTION

In our day-to-day lives, the use of plastics is being increased. Many of these plastics are made of synthetic materials. Because of their lack of biodegradable properties, these plastics do not degrade into soil and, therefore, cause environmental problems. In recent years, many developments in bioplastics[1] have been made to minimize the ill effects caused by synthetic plastics. Starch is a natural polymer, and it is versatile, cheap, and abundant in nature. It is currently used in coatings and sizing in paper, textiles, carpets, binders, adhesives, adsorbents, and encapsulates in the food industry.[2] Poly(methyl methacrylate) (PMMA) is a clear, colorless, and odorless polymer. It also has a good impact strength, higher than that of glass and polystyrene and lower than that of polycarbonate.[3] PMMA swells and dissolves in many organic solvents; it has a poor resistance to many other chemicals[4] on account of its easily hydrolyzed ester groups. Its environmental stability is superior to most other plastics, such as polystyrene and polyethylene. PMMA is, therefore, often the material of choice for outdoor applications.[5] It is useful in aircraft windows, protective coatings, lenses, dentures, transparent domes in automobiles, light shades, and sign boards. Many researchers have reported the biodegradability of polymer/starch composites.[6] The graft copolymerization of methyl methacrylate onto starch showed high superabsorbency properties.[7] The biodegradabilities of various polymers, including poly(vinyl alcohol), poly(hydroxyl alkanoate)s, and polylactide, have been increased through their incorporation of starch.[8]

The use of thin plastic sheets has increased in many domestic and industrial applications. In those applications with various modes of loading, mode I (in-plane) cracking is a common failure mode.[9] Resistance to fracture is the most important mechanical property of flexible materials, such as thin polymer sheets. The method of essential work of fracture (EWF) is used to determine the toughness of thin plastic films.[10–12] The importance of this method is that it deals with the sort of gross ductility that can occur in the plane stress fracture state. In EWF theory, there is dissimilarity between the inner process zone (process plane), where the actual crack runs, and the plastic zone, which surrounds the process zone. The total work needed to fracture a precracked specimen can be divided into two parts: the essential work of fracture (W_e) and the nonessential or plastic work of the fracture (W_p), W_e is the energy

needed for the yielding of the inner fracture process zone, and W_p is the work done in the yielding of the outer plastic zone and the actual energy dissipated in the outer plastic region, where various types of deformations may take place. W_e is a surface-related parameter, whereas W_p is a function of the deformed plastic zone volume. In earlier studies,[13] two-zone EWF models were developed to determine the tear fracture resistance of polymer thin films. Subsequently, a three-zone model was proposed by Kim and Karger-Kocsis[14] to analyze the out-of plane trouser tear fracture of ductile polymer films. For mode I (in-plane) loading, an EWF model was developed to characterize the fracture zone of PMMA and PMMA/starch composite films. In all of these cases, EWFs of various ductile polymers were determined.[15] However, no one has attempted to investigate the EWF of partially ductile materials, such as PMMA/starch composites. The toughness, along with biodegradability, of PMMA may be enhanced by the incorporation of starch into it. This novel combination could have emerging applications in the automobile and packing industries. The EWF method provides us with a technique for obtaining parameters for the partially ductile fracture toughness process.

THEORETICAL CONSIDERATIONS

The total work of fracture (W_t) for a precracked sample, in the double-edged notched tension (DENT) geometry, as shown in Figure 1, under mode I loading can be divided into two components:

1. Total work of fracture (W_t)

$$W_t = 2(W_e + W_p) \tag{1}$$

2. Specific total work of fracture (w_t)

$$w_t = 2(w_e + w_p \beta l) \tag{2}$$

where w_e is the specific essential work of fracture, w_p is the specific nonessential work of fracture, β is the shape factor for the outer plastic zone,[16] and t is the specimen thickness. A schematic

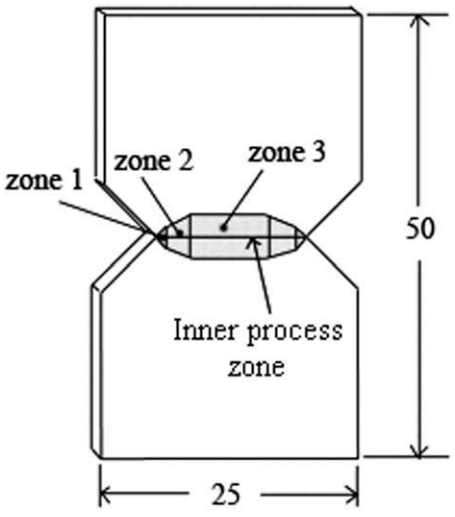

Figure 1. Fractured zone of the DENT specimens having two zones, namely, an inner process zone and an outer plastic zone.

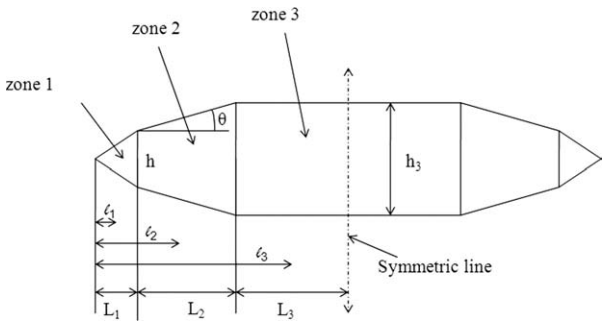

Figure 2. Crack zone (model) divided into three zones, depending on crack propagation.

showing the three zones (1–3) for the outer plastic zone is given in Figure 2 (where l_1, l_2, and l_3 are variable lengths; L_1, L_2, and L_3 are fixed lengths of the respective zones; h and h_3 are the heights of zones 1 and 3, respectively; and θ is the inclination angle of zone 2). It has been shown that the w_e's determined from zones 1–3 model are identical because w_e is a geometry-independent parameter.

The total work of fracture in zone 1 (W_{1t}; $0 < l_1 < L_1$) is given by

$$W_{1t} = 2(W_{1e} + W_{1p}) \tag{3}$$

where the subscripted numbers indicate the zone number. Equation (3), in terms of specific fracture work, is given by

$$W_{1t} = 2(w_{1e} l_1 t + w_{1p} A_1 t) \tag{4}$$

$$W_{1t} = 2(w_{1e} l_1 t + w_{1p} l_1^2 t) \tag{5}$$

where A_1 denotes the area of zone 1. Its profile inclination was assumed to be approximately 45° to the propagation path.[17] The specific total work of fracture in zone 1 (w_{1t}) becomes

$$w_{1t} = (w_{1e} + w_{1p} l_1) \tag{6}$$

where $w_{1t} = W_{1t}/2l_1 t$. The same methodology used for zone 1 was adopted for zone 2 ($0 < l_2 < L_1 + L_2$), where eq. (6) becomes

$$w_{2t} = w_{2e} + w_{2p}\left(\frac{L_1^2 + 2L_1 l_2 + \alpha l_2^2}{L_1 + l_2}\right) \tag{7}$$

The inclination angle (α) is calculated as follows:

$$\alpha = \frac{h_3 - 2l_1}{2L_2} \tag{8}$$

For zone 3 ($0 < l_3 < L_1 + L_2 + L_3$), eq. (6) becomes

$$w_{3t} = w_{3e} + w_{3p}\left(\frac{L_1^2 + 2L_1 L_2 + \alpha L_2^2 + h_3 l_3}{L_1 + L_2 + l_3}\right) \tag{9}$$

The total work of fracture in zone 3 (W_{3t}) could be determined by the calculation of the integral of the force–displacement curve area obtained from the tensile tests performed on the

Table I. Mechanical Strengths of the Biodegradable Samples at the Initial Time and after 8 Weeks

Composition	Initial value		Value after 8 weeks	
	Tensile stress at maximum load (MPa)	Total elongation (%)	Tensile stress at maximum load (MPa)	Total elongation (%)
Pure PMMA	38.41	12.21	34.48	11.68
PMMA + 2 wt % starch	36.57	17.24	32.24	9.24
PMMA + 4 wt % starch	35.59	19.82	29.83	7.43
PMMA + 6 wt % starch	34.08	22.77	27.46	5.75
PMMA + 8 wt % starch	32.49	24.36	25.07	4.06

DENT specimens of various ligament sizes. From eq. (9), w_{3e} and w_{3p} were determined by linear regression analysis[18] with a plot of w_{3t} versus $\left(\frac{L_1^2 + 2L_1L_2 + \alpha L_2^2 + h_3l_3}{L_1 + L_2 + l_3}\right)$. The lengths and heights of the cracked zone were determined with an optical microscope.

EXPERIMENTAL

Materials

Microsized potato starch powder (moisture = 18.5%, whiteness = 91.10%) had an average particle diameter of 35–60 μm. Dichloromethane (DCM) was supplied by Chemind Chemicals (Calicut, Kerala). PMMA (LG Chemical IH830-PMMA) clear-type granules were supplied by Vijaya Lakshmi Polymers Pvt., Ltd. (Bangalore, India).

Preparation of the PMMA/Starch Composites

PMMA was dissolved in DCM with a concentration of 200 mg/mL. The mixture was mechanically stirred for 1 h to completely dissolve PMMA. Various weight percentages of microsized starch were dispersed in PMMA liquid solution and stirred for 30 min to achieve final dry composites containing 0, 2, 4, 6, and 8 wt % concentrations of starch particles in the PMMA matrix. Finally, the synthesized PMMA/starch composites were dried in glass molds at room temperature for 24 h. With the starch powder at loading levels of 0–8 wt %, a series of composite sheets with thicknesses of about 0.9 mm were prepared.

Preparation of the DENT Specimens

Eight samples each of pure PMMA and PMMA/starch (2 wt % starch) composites were used to prepare the DENT specimens (Figure 2). We used the PMMA/2 wt % starch because composites having a starch content of 2 wt % showed higher values of tensile strength and percentage elongation than the other composites, which had 4–8 wt % starch. Each specimen was cut with a sharp razor blade to different ligament lengths from 9 to 16 mm.[19] Ideally, ligament lengths should be within the range of a $3t - 5$ mm (minimum) $< l < W/3$ (maximum),[20] where W, l, and t are the width, ligament length, and thickness of the DENT specimen, respectively.

Characterization

The mechanical and EWF properties were investigated with an Instron universal testing machine (model H10KS). Interatomic interactions of the starch with the polymer matrix were studied by Fourier transform infrared (FTIR) spectroscopy. The PMMA/starch composites were ground into powder form with a pestle with the application of uniform pressure. The IR spectra of the PMMA and PMMA/starch composites in the form of KBr pellets were recorded with an FTIR spectrometer (Bruker FTIR tensor model 27 spectrometer). The IR spectrum was recorded in transmission mode. The morphology and dispersion of starch in PMMA were investigated with scanning electron microscopy (SEM) with SU 6600 model instrument (Hitachi, Calicut, Kerala). Thermogravimetric analysis (TGA) was conducted on a TA Instruments Q-50 instrument. A small portion of the composite sample, approximately 10 mg (PMMA and PMMA/starch), was taken for TGA (Calicut, Kerala).

RESULTS AND DISCUSSION

Mechanical Characterization

The tensile strength of the PMMA/starch composites was found decrease as the starch content increased (Table I), and the percentage elongation of the composites increased up to a starch content of 8 wt %. Composites having a starch content of 2 wt % showed a decrease in tensile strength of 1.84 MPa and an increase in the elongation of 5.03% compared with those of the pure PMMA. The composite samples having starch contents of 4–8 wt % were not considered for further investigation because of their lower strength, which was caused by large agglomerations of starch in the PMMA matrix (Figure 3).

Biodegradability

The composite samples were cut to have dimensions of 10 × 10 cm^2. The initial tensile strength of each sample was measured. The samples of PMMA and PMMA/starch were placed in virgin soil under normal atmospheric conditions. The samples were placed in the soil at a depth of 5 cm. A similar methodology was adopted by earlier researchers.[21] Samples were buried in the soil for 8 weeks. The samples were taken out of the soil after 8 weeks and washed with distilled water. The tensile strength was measured after the samples were dried in a vacuum oven at room temperature. The decreases in the tensile strength and percentage elongation of the samples that were subjected to the soil burial test are shown in Table I. The decreases in the tensile strength and percentage elongation were higher in the composites having greater starch contents. It was clear that the tensile strength decreased with aging. The tensile strength decreased because of the degradation of starch particles in the PMMA sheets. This showed the biodegradability of the composites. The polarity of starch molecules might have helped accelerate the microbacterial attack on the composites, which resulted in the breakdown of the composite structure.

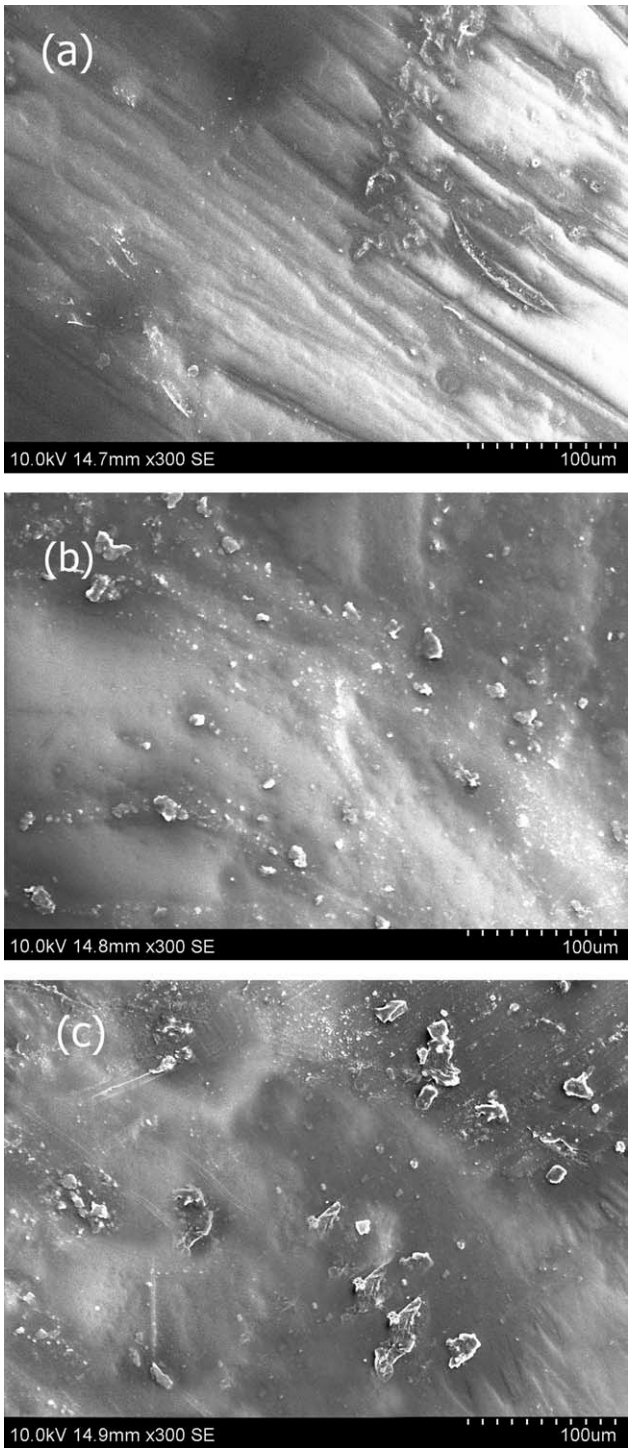

Figure 3. SEM images of (a) PMMA, (b) PMMA/starch composite (2 wt % starch), and (c) PMMA/starch composite (8 wt % starch).

FTIR Spectroscopy

The FTIR spectra indicated the details of functional groups present in the synthesized virgin PMMA and PMMA/starch composites, as shown in Figure 4. A thin (10-μm) PMMA/starch composite, virgin starch, and pure PMMA samples were prepared for FTIR analysis. From the FTIR spectra of starch, a strong and broad peak at 3326 cm^{-1} was assigned to the characteristic absorption peak due to the stretching vibrations of —OH. The wide absorption band at 3282 cm^{-1} of the PMMA/starch composite indicated the presence of H-bonded —OH groups on the surface of the PMMA/starch composite. The reduction of O—H stretching from 3326 to 3282 cm^{-1} may have been due to the hydrogen bonding between the O—H group of starch and PMMA.[22] A sharp absorption peak at 1725 cm^{-1} appeared and was due to the presence of ester carbonyl (C=O) stretching vibrations in the starch; this peak was also present in the same position in the FTIR spectra of the PMMA/starch composites. There was a peak shift toward lower frequencies from 2922 to 2845 cm^{-1} with the addition of the starch into PMMA; this appeared to be due to the presence of C—H stretching vibrations.[23]

SEM

The fractured surface morphology of the PMMA composites having 2 and 8 wt % starch was examined through SEM. The dispersion of starch within PMMA is shown in Figure 3. It was found that starch particles were distributed with an average diameter of 30 μm, and a more uniform distribution of particles appeared in the 2 wt % starch composites than in the composites having 8 wt % starch. So, when the starch content was increased in the PMMA matrix, larger starch particles were recognized. This may have been due to the agglomeration[24] of starch particles during the synthesis process.

TGA

The thermal properties of the PMMA/starch composites were studied by TGA. The TGAs of PMMA and PMMA/starch composites in the temperature range from 100 to 800°C are compared in Figure 5. The degradations of the PMMA and PMMA/starch composites having starch contents of 2–8 wt % started at 333, 337, 341, 345, and 348°C, respectively. The PMMA/starch composites had higher thermal stabilities than pure PMMA. Because the melting point of PMMA was 225°C and that for starch was 260°C, as the starch content was increased in the composites, the thermal decomposition temperature increased from 305 to 348°C. This clearly highlighted the advantage of

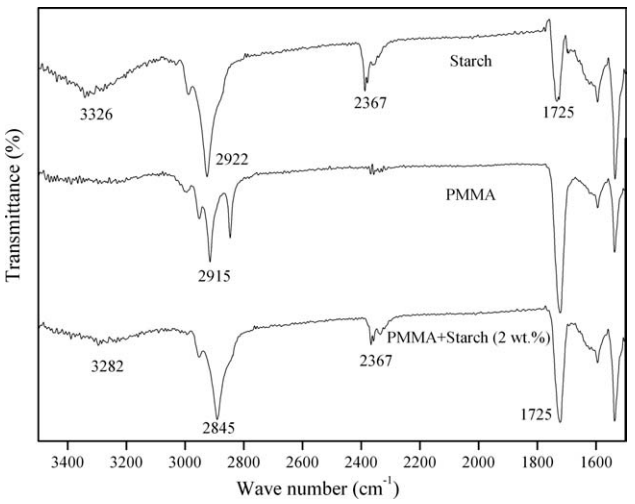

Figure 4. FTIR spectra showing functional groups present in the pure PMMA and PMMA/starch composite (2 wt % starch).

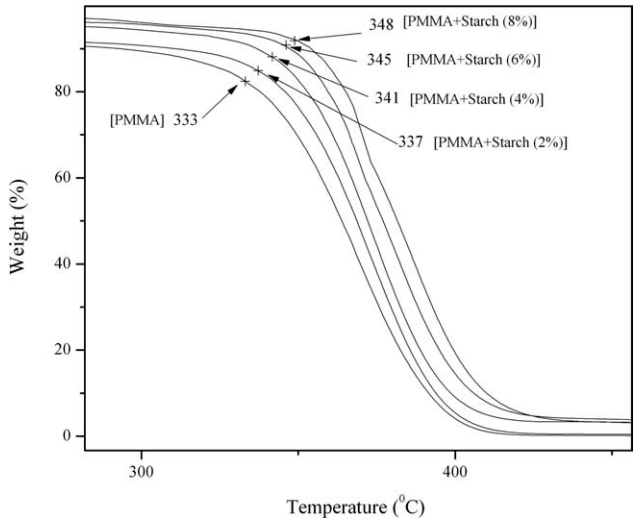

Figure 5. Increase in the decomposition temperature as the starch content increased in the composites.

the reinforcement.[25] For pure PMMA, the onset degradation started at 305°C with a weight loss of 6%, and for the composite sample having a starch content of 8 wt %, it started at 348°C with a weight loss of 3%. Thermograms revealed that the thermal stability of the composites increased as the filler content increased.

EWF

Tensile tests were performed on DENT specimens with various ligament sizes, as shown in Figure 6. The force–displacement graphs were determined by the Instron H10KS universal testing machine. The strain rate was fixed at 1 mm/min.[26]

For pure PMMA, the maximum load and the displacement at failure also increased with increasing ligament length, as shown in Figure 7(a). This showed that the pure PMMA fulfilled one of the basic requirements of the EWF method. It also ensured that the pure PMMA showed partial ductile fracture behavior.[27] This may have occurred because of the effect of the solvent (DCM) on the PMMA films prepared by the solvent casting

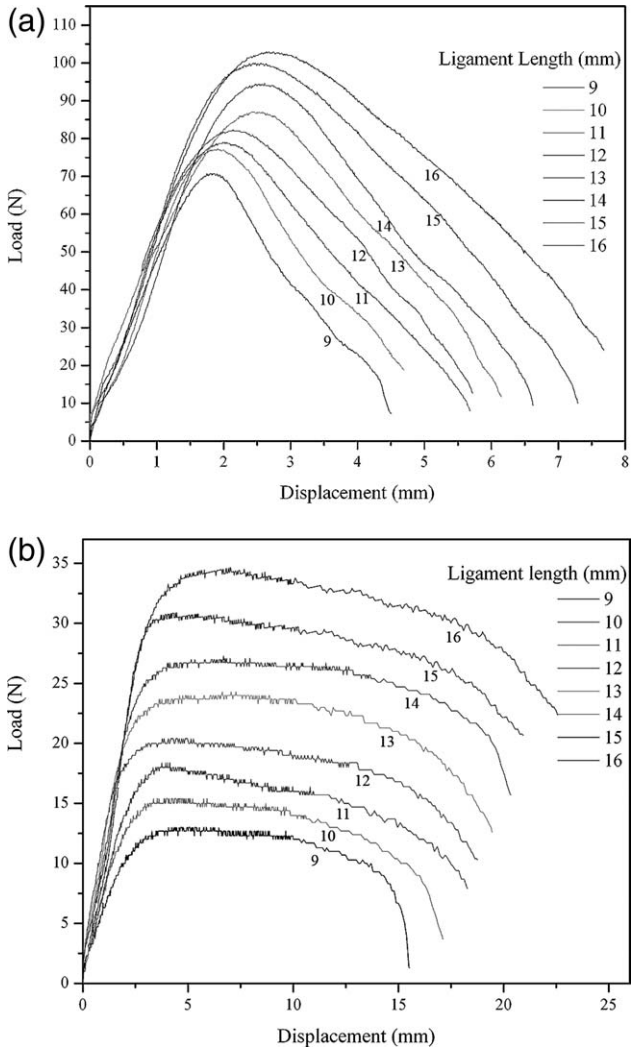

Figure 7. Load–displacement curves obtained from tensile testing on the Instron testing machine: (a) pure PMMA and (b) PMMA/starch composite (2 wt % starch).

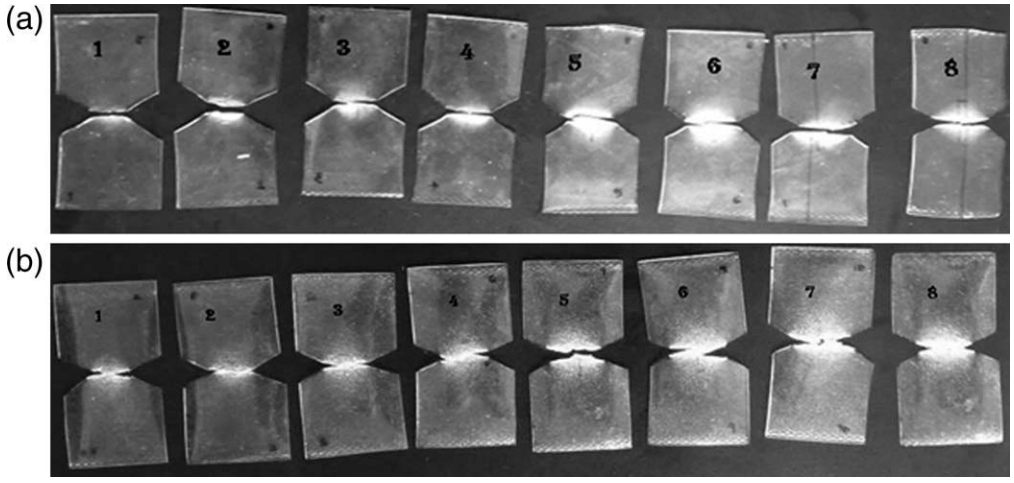

Figure 6. Increase of the outer plastic zone in the DENT specimens: (a) pure PMMA and (b) starch content = 2 wt %.

Applied Polymer SCIENCE

Table II. Experimental Values of the Ligament Length and W_t

Ligament length (mm)		W_t (J)	
Pure PMMA	Starch (2%)	Pure PMMA	Starch (2%)
7.96	8.45	175.03	165.87
9.3	9.17	180.78	205.08
10.03	9.9	272.8	256.64
11.28	11.02	309.56	281.35
12.18	12.21	335.29	417.45
12.92	12.96	424.06	452.31
13.74	13.94	523.95	453.38
14.82	14.84	656.13	620.95

technique. The area under the force–displacement of each curve was measured by Origin 8 statistical software (Originlab, Calicut, Kerala).

An important prerequisite of the plane stress EWF approach is that the crack propagates only after the ligament has been fully yielded. With eq.(9), the equivalent ligament length (L^*) parameters were measured with optical microscopy. The measured ligament length values and corresponding W_t's are shown in Table II.

The w_t versus L^* plot is shown in Figure 8. The intercept of the y axis gave w_e, and the slope indicated w_p.

The w_e value of pure PMMA was found to be 4.559 KJ/m^2 and that of the PMMA/2 wt % starch composite was 8.129 KJ/m^2, as listed in Table III.

ANSYS (Calicut, Kerala) Simulation

The determination of the essential fracture work of composites by the experimental procedure consumes much more time because of the very low feed rate (1 mm/min) given with the tensile testing conditions. This time consumption and testing costs have led to a need for alternative procedures. ANSYS simulation is an effective way to determine the EWF of composites. In the ANSYS simulation, the samples were modeled with similar dimensions, boundary conditions, and loadings as in the experimental procedure. A plane 82 element was chosen for the analysis because of its high deformations and plasticity properties. Because of the axisymmetry of the sample, one-quarter of the whole sample was modeled. The arc-length method was used to control the nonlinear solution because it could also solve the negative slopes. By changing the ligament length of the samples, we calculated the plastic equivalent stress and equivalent plastic strains. The time-history step allowed us to provide the plastic equivalent stress versus equivalent plastic strains plots. These plots gave us sufficient data to determine W_t after the yield point. The measured ligament length values and corresponding W_t values are shown in Table IV.

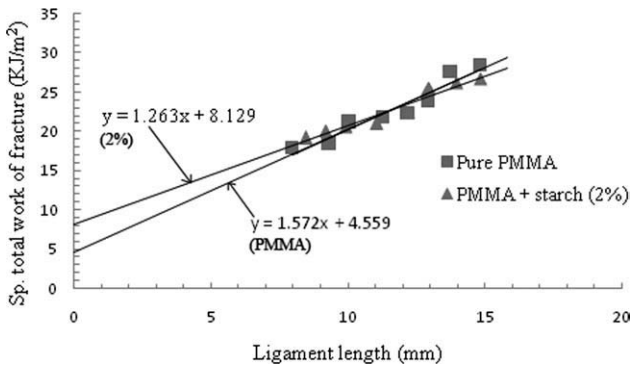

Figure 8. L^* versus w_t plot obtained by the experimental method.

Table III. w_e and βw_p Values Obtained by EWF Analysis

Composition	w_e (kJ/m^2)	βw_p (MJ/m^3)
Pure PMMA	4.559	1.572
PMMA + 2 wt % starch	8.129	1.263

The stress–strain values obtained by ANSYS were converted into load–displacement. The load–displacement curves for the PMMA and PMMA composites with 2 wt % starch are shown in Figure 9.

The intercept of the y axis was the measurement of EWF, as shown in Figure 10.

w_e of pure PMMA was found to be 4.052 KJ/m^2, and that of the PMMA/2 wt % starch composite was 7.074 kJ/m^2. w_p of pure PMMA was found to be 1.244 MJ/m^2, and that of the PMMA/2 wt % starch composite was found to be 1.103 MJ/m^2, as listed in Table V. The fracture values obtained by the ANSYS simulation were lower than the experimental values because, in ANSYS, the convergence of the solution was possible only up the break point load of the specimen. This resulted in a reduction of the area under the load–displacement curve and, thereby, a reduction in the work required to fracture.

Through a comparison of w_e of the experimental and simulation values, the percentage variation for the pure PMMA was 12.97%, and the percentage variation for composites with 2 wt % starch was 11.12%.

CONCLUSIONS

A novel composite system based on natural reinforcements, such as potato starch, was prepared. The tensile strength of the PMMA/starch composites was found to decrease as the starch

Table IV. ANSYS Simulation Values of L^* and W_t

L^* (mm)		W_t (J)	
Pure PMMA	Starch (2%)	Pure PMMA	Starch (2%)
9	9	145.52	158.69
10	10	175.68	195.81
11	11	223.56	232.52
12	12	260.39	278.26
13	13	315.30	335.68
14	14	423.76	435.56
15	15	463.81	473.56
16	16	515.82	520.43

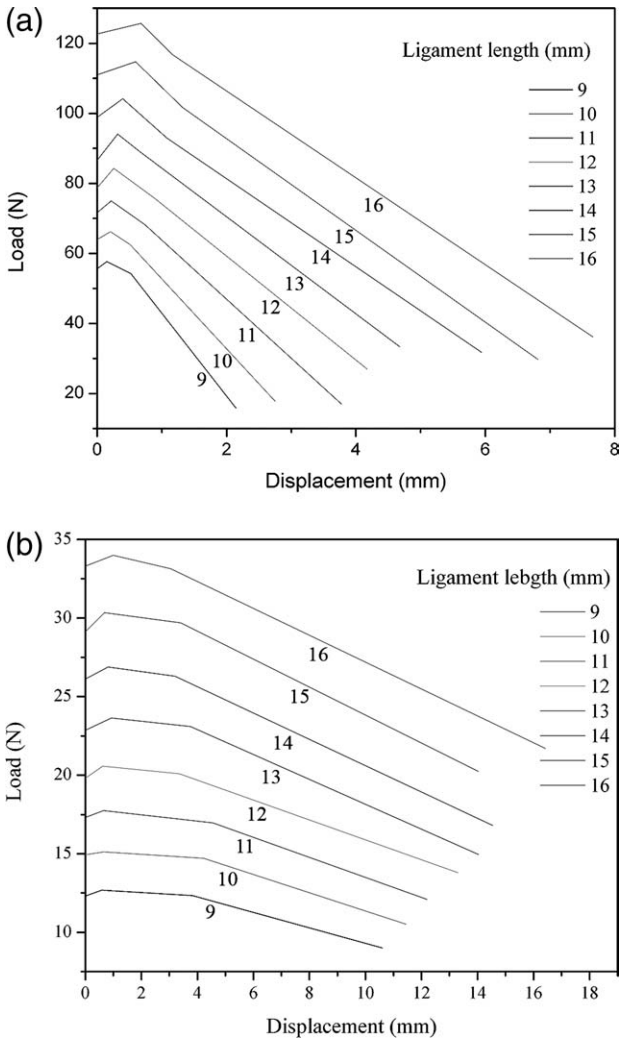

Figure 9. Load–displacement curves obtained from the ANSYS software for the (a) pure PMMA and (b) PMMA/2 wt % starch composites.

content increased, but sufficient strength was maintained by composites having starch contents of up to 2 wt %. The total elongation of the composites increased as the starch content increased. From the FTIR spectra, we observed that after the addition of starch to PMMA, the broad peak in the O—H and

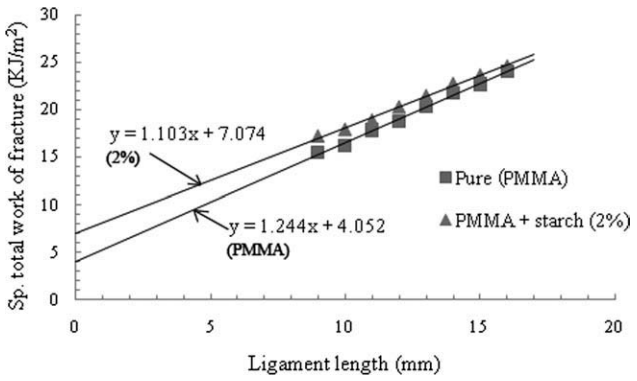

Figure 10. L^* versus w_t plot obtained by the ANSYS software.

Table V. w_e and βw_p Values Obtained by the ANSYS Simulation

Composition	w_e (kJ/m^2)	βw_p (MJ/m^3)
Pure PMMA	4.052	1.244
PMMA + 2 wt % starch	7.074	1.103

C—H boding regions shifted to a lower frequency. This shift revealed that there was intermolecular interaction between the PMMA and starch. The biodegradability of the composites was found to increase with increasing starch content. TGA showed that the increase in the starch content in the composites increased the thermal decomposition temperature. The plane stress fracture behavior of the PMMA/starch composites was studied by the EWF method and ANSYS simulation with DENT specimens in this study. The EWF analysis showed that the w_e values of the composites was independent of the geometry, and they increased up to 1.78 times that of the pure PMMA samples. In the ANSYS simulation, the w_e values of the composite sample with a starch content of 2 wt % increased up to 1.74 times that of the pure PMMA samples.

REFERENCES

1. Lu, D. R.; Xiao, C. M.; Xu, S. *J.Express Polym. Lett.* **2009,** *3*, 366.
2. Thakore, I. M.; Desai, S.; Devi, S. *Int. J. Polym. Mater.* **2003,** *52*, 725.
3. Yuan, Y. L.; Wu, C. M. L.; Li, R. K. Y. *Polym. Test.* **2007,** *26*, 102.
4. Masahito, Y. T. *Surf. Coat. Technol.* **2009,** *203*, 2587.
5. David, C.; Miller, S. R. *Sol. Energy Mater. Sol. Cells* **2011,** *95*, 2037.
6. Greizerstein, H. B.; Joseph, A.; Paul, J. K. *Polym. Degrad. Stab.* **1993,** *32*, 251.
7. Prafulla, K.; Sahoo, P.; Rana, K. *J. Mater. Sci.* **2006,** *41*, 6470.
8. Ishigaki, T.; Kawagoshi, Y.; Ike, M.; Fujita, M. *World J. Microbiol. Biotechnol.* **1999,** *15*, 321.
9. Barany, T.; Ronkay, F.; Karger-Kocsis, J.; Czigany, T. *Int. J. Fracture* **2005,** *135*, 251.0
10. Pascual, L. A.; Beeman, S. C. *J. Angle Orthodontist* **2010,** *80*, 2319.
11. Bureau, M. N. *Eng. Fracture Mech.* **2006,** *73*, 2360.
12. Wu, J.; Mai, Y. *Polym. Eng. Sci.* **1996,** *36*, 2275.
13. Aksel, C.; Warren, P. D. *Compos. Sci. Technol.* **2003,** *36*, 1433.
14. Kim, H. S.; Karger-Kocsis, J. *Acta Mater.* **2004,** *52*, 3123.
15. Janet, S. S.; Wong, A.; Ferrer Balas, D. *Acta Mater.* **2003,** *51*, 4929.
16. Kocsis, K. *J. Polym. Bull.* **1996,** *37*, 119.
17. Sharon Kao-Walter, M. H.; Mats Walter, A. L. Presented at the 12th International Conference on Fracture, Ottawa, Canada, **2009.**

18. Pegoretti, A.; Castellani, L. *Eng. Fracture Mech.* **2009,** *76*, 2788.
19. Martinez, A. B.; Segovia, A. *Eng. Fracture Mech.* **2009,** *76*, 1247.
20. Lauke, B.; Schuk, T. *Int. J. Adhes. Adhes.* **2001,** *21*, 55.
21. Kaczmarek, H.; Bajer, K. *J. Polym. Sci. Part B: Polym. Phys.* **2007,** *45*, 903.
22. Grande, C. J.; Torres, F. G.; Gomez, C. M.; Troncoso, O. P.; Canet-Ferrer, J.; Martínez-Pastor, J. *Mater. Sci. Eng. C* **2009,** *29*, 1098.
23. Espigaresa, I.; Elvira, C.; Mano, J. F.; Vázquez, B.; Román, J. S. *Biomaterials* **2002,** *23*, 1883.
24. Aichayawanich, S.; Nopharatana, M.; Nopharatana, A.; Songkasiri, W. *Carbohydr. Polym.* **2011,** *84*, 292.
25. Zhou, X.; Yang, J. *J. Mater. Process. Technol.* **2009,** *209*, 5394.
26. Barany, T.; Czigany, T. *Periodica Polytech. Ser. Mech. Eng.* **2003,** *47*, 91.
27. Martinez, A. B.; Gamez-Perez, J.; Sanchez-Soto, M. *Eng. Failure* **2009,** *36*, 2604.